

Lifetimes of Rotational Levels in Some Odd-*A* Nuclei Measured by a Microwave Method

A. E. BLAUGRUND, Y. DAR, AND G. GOLDRING

Department of Physics, The Weizmann Institute of Science, Rehovoth, Israel

(Received June 1, 1960; revised manuscript received August 15, 1960).

Measurements of mean lives of the first excited states of a number of odd-*A* nuclei have been carried out with the intention of obtaining more accurate information on magnetic transition probabilities than is at present available. Most of these mean lives are in the range of $2-20 \times 10^{-11}$ sec, and for this measurement a special timing apparatus has been devised which consists of a microwave beam pulsing system and a beta-ray spectrometer and cavity combination which acts as a microwave shutter. In four cases the exponential decay could be determined directly; these were the first excited states of Lu^{175} , Hf^{179} , and Ta^{181} , and the 118-keV level of Tm^{169} . The results for these levels are: $\tau(\text{Tm}^{169}) = (9.0 \pm 0.4) \times 10^{-11}$ sec, $\tau(\text{Lu}^{175}) = (14.6 \pm 1) \times 10^{-11}$ sec, $\tau(\text{Hf}^{179}) = (5.4 \pm 0.4) \times 10^{-11}$ sec, and $\tau(\text{Ta}^{181}) = (6.0 \pm 0.5) \times 10^{-11}$ sec. Lifetime measurements were also carried out for the first excited states of Hf^{177} , Re^{185} , and Re^{187} . The limitations and scope of this method of measuring lifetimes are discussed.

INTRODUCTION

THE determination of *M1* transition probabilities between rotational levels in odd-*A* nuclei is important because according to current theories¹ the *M1* transition probabilities, together with the magnetic moment of the ground state (or any other level in the rotational band) essentially determine the value of g_R —the gyromagnetic ratio of the rotational motion. A systematic measurement of g_R throughout the region of rotational nuclei would be of interest, in particular in relation to gyromagnetic ratios of even-even rotational nuclei. An even more fundamental problem is whether the description of the static moments and transition moments throughout the rotational band in terms of two parameters g_R and g_Ω —the gyromagnetic ratio of the nucleon configuration—is actually valid. The electric quadrupole moments do indeed conform quite well to such a description in terms of a single parameter Q_0 , and the individual levels and transitions differ only in their geometric rotational properties.² However, until the nature of the rotational motion is more clearly understood one cannot be certain that similar relations actually hold for *M1* transitions as well. It is, for example, conceivable that the nuclear configuration changes slightly from one level to another. These changes may be small enough not to affect the collective quadrupole moment and yet have an appreciable effect on g_Ω which then would not be a constant of the band. It seems that in any case the constancy of g_Ω is a much more rigorous proof of the purity of the collective motion than the constancy of Q_0 and for this reason we expect the measurement of magnetic dipole moments to provide a more sensitive means for the detailed investigation of the structure of rotational nuclei than electric quadrupole moments. It is therefore of prime importance to investigate directly the consistency of the description of all

magnetic dipole quantities in terms of g_R and g_Ω , for example by measuring *M1* transition probabilities for two different transitions. Measurements to date³ indicate that for several nuclei the *M1* transition probabilities for the transition from the first excited state to the ground state and from the second excited state to the first excited state are indeed consistent with one fixed value of $(g_R - g_\Omega)^2$. However, in most of these measurements the *M1* transition probability is deduced from the *E2* transition probability and the mixing ratio $\delta^2 = E2/M1$, and these measurements are not accurate enough to be conclusive, because in order to determine the mixing ratio δ^2 , all these measurements rely on the determination of some quantity x (e.g., anisotropy in the angular distribution of γ rays, total conversion coefficient, *K/L* ratio) which has different and well known values for pure *E2* and *M1* transitions and which in mixed transitions has a mean value, weighted according to the relative amounts of *M1* and *E2*. δ^2 can be determined from the measured value of x by means of the relation:

$$x(\delta^2) = \frac{\delta^2 x(\infty) + x(0)}{\delta^2 + 1} F.$$

For the *K/L* ratio δ^2 has to be replaced by δ^{2*}

$$\delta^{2*} = \delta^2 \frac{\alpha_L(E2)}{\alpha_L(M1)}$$

where α_L are the *L*-conversion coefficients for pure transitions.

Most of the transitions in the odd-*A* nuclei are predominantly *M1*, with $\delta^2 \ll 1$ and one sees that in this case:

$$\frac{d\delta^2}{\delta^2} \sim \frac{1}{\delta^2} \frac{x(0)}{x(\infty) - x(0)} \frac{dx}{x},$$

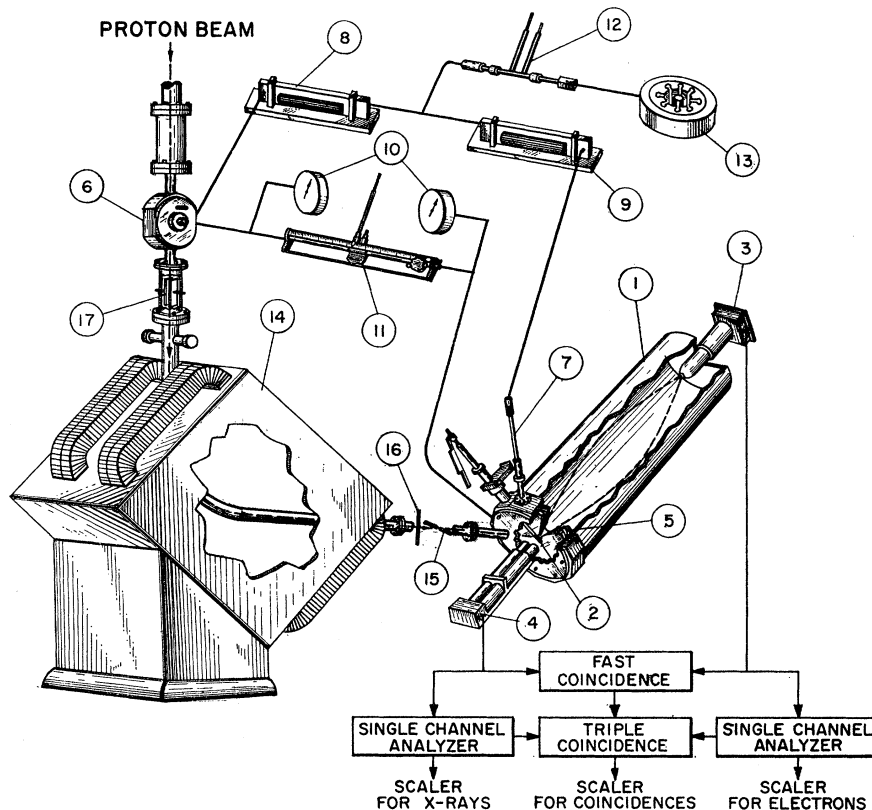
and therefore the sensitivity of this type of measurement

¹ A. Bohr and B. R. Mottelson, *Kgl. Danske Videnskab. Selskab, Mat.-fys. Medd.* **27**, No. 16 (1953).

² G. Goldring and G. T. Paulissen, *Phys. Rev.* **103**, 1314 (1956).

³ J. de Boer, M. Martin, and P. Marmier, *Helv. Phys. Acta* **32**, 377 (1959). In this paper previous work is also summarized.

FIG. 1. Schematic drawing of the apparatus. (1) β -ray spectrometer; (2) target; (3) electron counter; (4) x-ray counter; (5) energy modulating cavity; (6) beam pulsing cavity; (7) line stretcher for phase adjustment between cavities; (8,9) unilines; (10) meters for cavity outputs; (11) interferometer for checking the phase between the cavities; (12) double stub transformer; (13) magnetron; (14) deflection magnet; (15) beam chopping slit; (16) slit for energy stabilization; (17) 50 cycle/sec deflection plates.



becomes very low. It is obviously preferable to measure some quantity in which the contributions from $E2$ and $M1$ transitions add (instead of being averaged). The transition probability itself (or its inverse—the mean life) is such a quantity, for we have:

$$\frac{1}{\tau} = \frac{1}{\tau_{M1}} + \frac{1}{\tau_{E2}},$$

or

$$\frac{1}{\tau} = \frac{1 + \alpha}{\tau_{\gamma, M1}} (1 + \delta^2),$$

where α is the total conversion coefficient and $\tau_{\gamma, M1}$ is the partial mean life for $M1$ γ emission. For low δ^2 a measurement of τ is an almost direct determination of $\tau_{\gamma, M1}$: the value δ^2 has to be known only roughly.

Lifetime measurements in these transitions have not so far been carried out because the transitions are rather fast, 10^{-11} – 10^{-10} sec, and beyond the range of direct electronic measurements. In the present paper a new method is described which has been developed for the measurements of these short lifetimes. In this method the necessary high time resolution is achieved by means of a microwave beam pulsing and timing device.

Similar measurements, based on the same timing devices have been carried out previously⁴ with radio-

active sources. In those measurements severe limitations had to be faced which were largely overcome in the present beam pulsing measurements.

Transitions from the first excited state to the ground state were investigated in Lu^{175} , Hf^{177} , Hf^{179} , Ta^{181} , Re^{185} , and Re^{187} , and the 110-keV transition in Tm^{169} . It is hoped that in future measurements the lifetimes of higher excited states can be determined, thus making it possible to check the constancy of $(g_R - g_\alpha)^2$ within a rotational band.

EXPERIMENTAL ARRANGEMENT

The general experimental arrangement is shown in Fig. 1. The target nuclei are excited by Coulomb excitation with protons of 2.5 MeV from a 3-MeV High Voltage Engineering Corporation Van de Graaff accelerator. The proton beam passes through a microwave cavity, shown in detail in Fig. 2(a). The cavity is fed from a CW magnetron of 80 watts operating at 2450 Mc/sec. The electric field in the cavity is concentrated in the central region, between the post and the membrane and it produces a transverse force on the protons. The width of the post is such that the time it takes the protons to pass over it is slightly less than one half period ($T = 40.8 \times 10^{-11}$ sec). It was found that when about 30 watts are dissipated in the cavity the deflection has an amplitude of 10^{-3} radian. After the beam pulsing cavity, the beam passes through

⁴ A. E. Blaugrund, Phys. Rev. Letters 3, 226 (1959).

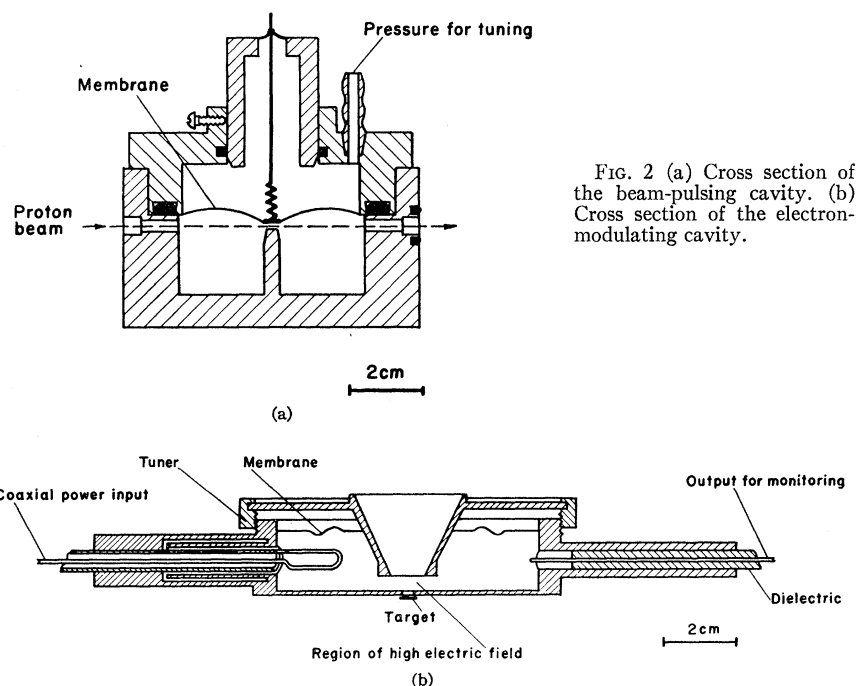


FIG. 2 (a) Cross section of the beam-pulsing cavity. (b) Cross section of the electron-modulating cavity.

the deflection magnet and on to a vertical slit 1 mm wide which chops the modulated beam. After that the beam hits the target. The length of path traversed by the protons between the deflection cavity and the target is 230 cm. The radiation coming off the target is time-analyzed by a shutter device which has already been briefly described elsewhere.⁴ The shutter consists of a lens-type β -ray spectrometer which is set to accept conversion electrons from the required transition and a microwave cavity which is located between the target and the spectrometer and which modulates the energy of the electrons. The spectrometer has a momentum resolution of 1% and a transmission of 2.2%. The electron-modulating cavity is fed from the same magnetron as the beam-pulsing cavity. When dissipating 30 watts this cavity produces a modulation of the electron energy with an amplitude of about 4 keV. The electron-modulating cavity is shown in detail in Fig. 2(b). The modulation throws most of the electrons out of focus except those which go through the cavity at the time when the microwave field is zero. The electrons which are recorded therefore have a definite phase with respect to the pulsed beam and therefore a time scale is established.

The decay of the excited state can be investigated if one counts electrons in the spectrometer as a function of the relative phase between the oscillations in the two cavities. In actual practice the phase was kept constant to ensure stable microwave operation and the variable time delay was achieved by changing the proton velocity. Only very small changes are required since a relative change of 4×10^{-3} in velocity already

covers a complete period. In most of the cases investigated in this work, the mean life was not much smaller than the microwave period and one therefore finds that excited nuclei produced by a given beam pulse have not all decayed by the time the next beam pulse hits the target. There are other unfamiliar properties of this type of time measurement which derive from the fact that both the beam pulse and the detector time-window have a repetition rate of $2/T$ (rather than $1/T$). In order to elucidate these points, a detailed analysis of the beam and counter modulating technique is given in the next section.

ANALYSIS OF MODULATION SYSTEM

Let x be the coordinate of the beam movement in the plane of the beam chopping slit. We define a function $g(x)dx$, "the beam profile," as the current falling between x and $x+dx$ if the center of gravity of the current distribution is at $x=0$. If the beam position is modulated with angular frequency ω and amplitude b then the current falling at time t between x and $x+dx$ will be given by

$$f(x,t)dx = g(x - b \sin \omega t)dx.$$

The current passing through a slit which extends from $x = -D/2$ to $x = D/2$, in the time t is given by

$$i(t) = \int_{-D/2}^{D/2} g(x - b \sin \omega t)dx.$$

We now define a function $G(x)$ —the "apparent beam

profile" as

$$G(x) = \int_{-D/2}^{D/2} g(x'+x) dx',$$

and we get

$$i(t) = G(-b \sin \omega t). \quad (1)$$

If in particular the amplitude of modulation b is much larger than both the beam diameter and the slit width then $i(t)$ will represent a train of current pulses spaced by time intervals $\frac{1}{2}T$.

Turning now to the spectrometer modulation we consider first the case of prompt radiation, i.e., radiation emitted immediately after the excitation of the nucleus ($\tau=0$).

The momentum spectrum of the electrons as measured in the spectrometer is $S(p)$: the number of electrons counted if the spectrometer is set to the value p , and if one unit of charge has fallen on the target. If a modulation $q \sin(\omega t - \varphi)$ is applied to the electron momentum, where φ is an arbitrary phase, the instantaneous spectrum at a time t will be given by⁵

$$S_i(p, t) = S(p - q \sin(\omega t - \varphi)).$$

If in particular $S(p)$ represents a well-defined line with a peak at p_0 , and if q is large compared to the electron linewidth, then $S_i(p_0, t)$ represents a train of electron bursts passing the modulating cavity at times $t = (k\pi + \varphi)/\omega$, where k is an integer.

If now the beam is modulated too, the number of electrons in the time interval $(t \cdots t + dt)$ will be proportional to $i(t)dt$, and in particular the number of electrons of momentum p in the time interval $(t \cdots t + dt)$ is given by

$$n(t)dt = i(t)S_i(p, t)dt = G(-b \sin \omega t) \times S(p - q \sin(\omega t - \varphi))dt. \quad (2)$$

The quantity which is actually measured is the integral of $n(t)$ over time keeping φ constant. We introduce a time Θ , very long compared to both T and τ , and define

$$N(p, \varphi) = \frac{1}{\Theta} \int_{-\Theta/2}^{\Theta/2} G(-b \sin \omega t) S(p - q \sin(\omega t - \varphi)) dt. \quad (3)$$

This is the number of electrons counted in unit time if the spectrometer is set to the momentum p , and the phase angle is φ .

If we consider $G(x)$ to be a very narrow function which differs from zero only very close to $x=0$, then for a given p , $N(p, \varphi)$ will be a periodic function of φ which in any period closely resembles the function $S(p)$. For example for small φ we have

$$N(p, \varphi) \sim S(p - q\varphi).$$

⁵ The microwave cavity actually modulates the energy rather than the momentum of the electrons, however if the modulation is small, i.e., $q \ll p$ then the energy change is proportional to the momentum change and there is no difference between energy and momentum modulation.

Even if $G(x)$ has a finite width this resemblance between $S(p)$ and $N(p, \varphi)$ (as a function of φ) will be preserved; $G(x)$ will merely broaden the spectrum. There is, however, an important difference between the two functions, namely: no matter what shape the function $S(p)$ has, $N(p, \varphi)$ will be a symmetric function of φ . For if we calculate $N(p, -\varphi)$ from (3) we get

$$N(p, -\varphi) = \frac{1}{\Theta} \int_{-\Theta/2}^{\Theta/2} G(-b \sin \omega t) S(p - q \sin(\omega t + \varphi)) dt,$$

and if we now introduce: $t' = \pi/\omega - t$ we get

$$N(p, -\varphi) = \frac{1}{\Theta} \int_{-\Theta/2+\pi/\omega}^{\Theta/2+\pi/\omega} G(-b \sin \omega t') \times S(p - q \sin(\omega t' - \varphi)) dt' = N(p, \varphi). \quad (4)$$

As indicated by the proof—the symmetry is a consequence of the fact that both the beam and the “shutter” recur every π radians. If the beam modulation is modified in some way so that the beam recurs only in 2π intervals, the symmetry is lost [unless both $G(x)$ and $S(p+x)$ are symmetric functions].

The function $N(p, \varphi)$ is evidently periodic in φ with period 2π . We now investigate whether it also has the period π . From (3) we get

$$N(p, \varphi + \pi) = \frac{1}{\Theta} \int_{-\Theta/2}^{\Theta/2} G(-b \sin \omega t) S(p + q \sin(\omega t - \varphi)) dt,$$

and we have

$$N(p, \varphi + \pi) = N(p, \varphi), \quad (5)$$

if either $G(x)$ or $S(p+x)$ (or both) are symmetric functions of x .

It will be shown later that the symmetry property (4) and the π periodicity (5) are of great importance for the analysis and interpretation of the measurements.

We now turn to the discussion of “delayed” radiation, i.e., radiation which after its initiation by the proton beam decays exponentially with mean life τ .

In analogy to (2) we get for the number of electrons of momentum p in the time interval $(t \cdots t + dt)$:

$$n_{\omega, \tau}(t) dt = S(p - q \sin(\omega t - \varphi)) \times \frac{1}{\tau} \int_0^{\infty} G(-b \sin \omega(t-t')) e^{-t'/\tau} dt', \quad (6)$$

where we have labeled n by both the decay constant and the modulation frequency. In a similar manner we get for the “ φ spectrum”—the integral of $n_{\omega, \tau}(t)$:

$$N_{\omega, \tau}(p, \varphi) = \frac{1}{\Theta} \int_{-\Theta/2}^{\Theta/2} n_{\omega, \tau}(t) dt = \frac{1}{\tau \Theta} \int_{-\Theta/2}^{\Theta/2} dt \times \int_0^{\infty} G(-b \sin \omega(t-t')) e^{-t'/\tau} \times S(p - q \sin(\omega t - \varphi)) dt'. \quad (7)$$

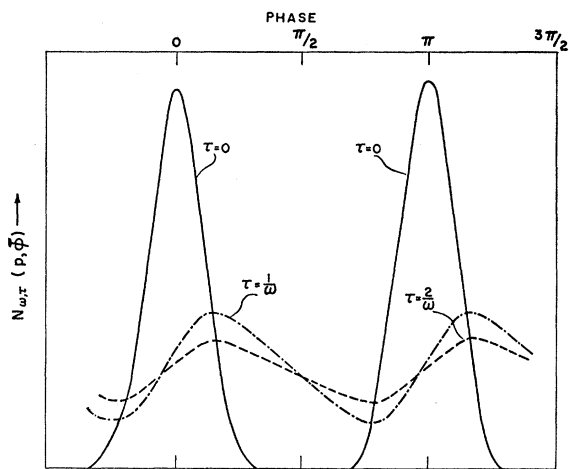


FIG. 3. Schematic drawing showing the relationship between $N_{0,\tau}(p,\varphi)$ and $N_{\omega,\tau}(p,\varphi)$.

Introducing the new variable φ' defined by $\varphi' = \varphi - \omega\tau$, we get

$$N_{\omega,\tau}(p,\varphi) = \int_{-\infty}^{\varphi} N(p,\varphi') \frac{e^{-(\varphi-\varphi')/\omega\tau}}{\omega\tau} d\varphi', \quad (8)$$

where $N(p,\varphi)$ is the function defined by (3). The significance of $N(p,\varphi)$ becomes clear if we let τ tend to zero. Since $\lim_{x \rightarrow 0} f(z)/x = \delta(z)$, where $f(z) = 0$ for $z < 0$ and $f(z) = e^{-z/x}$ for $z \geq 0$, we get: $N_{\omega,0}(p,\varphi) = N(p,\varphi)$ and therefore

$$N_{\omega,\tau}(p,\varphi) = \int_{-\infty}^{\varphi} N_{\omega,0}(p,\varphi') \frac{e^{-(\varphi-\varphi')/\omega\tau}}{\omega\tau} d\varphi'. \quad (9)$$

$N_{\omega,0}(p,\varphi)$ is the "prompt" response curve—the φ spectrum which would have been obtained for $\tau=0$. Equation (9) is very similar to the formulas commonly used in delayed coincidence work, with the important exception that instead of time measured in units of τ we have here a phase measured in units of $\omega\tau$. As a consequence of this we can also write Eq. (8) in the form:

$$N_{\omega,\tau}(p,\varphi) = \int_{-\infty}^{\varphi} N_{0,\tau}(p,\varphi') \frac{e^{-(\varphi-\varphi')/\omega\tau}}{\omega\tau} d\varphi'. \quad (10)$$

Here $N_{0,\tau}(p,\varphi)$ is the response curve for the same target which produces $N_{\omega,\tau}(p,\varphi)$ if the modulation is carried out with frequency $\omega \rightarrow 0$, all other parameters remaining the same. In other words—since only the product $\omega\tau$ is significant for the folding of $N_{\omega,\tau}(p,\varphi)$ into $N(p,\varphi)$, we can reproduce the prompt response by reducing either τ or ω ; the relevant criterion being that $\omega\tau \ll 1$.

The significance of (10) lies in the fact that $N_{0,\tau}(p,\varphi)$ can easily be measured by carrying out an experiment with low modulation frequency. It should be noted that for any given τ the function $N_{0,\tau}(p,\varphi)$ determines the function $N_{\omega,\tau}(p,\varphi)$ completely, without any arbitrariness, normalization, etc. The measurement of

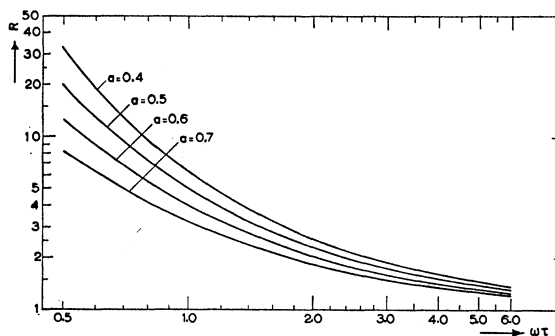


FIG. 4. The ratio R of the maximum value to the minimum value of $N_{\omega,\tau}(p,\varphi)$ if $N_{0,\tau}(p,\varphi) = N \exp(-\varphi^2/a^2)$. R is given as a function of $\omega\tau$ for different values of a .

both $N_{0,\tau}(p,\varphi)$ and $N_{\omega,\tau}(p,\varphi)$ therefore determines τ uniquely and rigorously.

For the practical determination of τ from the double measurement there are several possibilities, some of which will be discussed later on. At this point we wish only to point out some general properties of the relation between $N_{0,\tau}(p,\varphi)$ and $N_{\omega,\tau}(p,\varphi)$.

In Fig. 3 are shown very schematically the functions $N_{\omega,\tau}(p,\varphi)$ generated from a function $N_{0,\tau}(p,\varphi)$, by two different values of τ . We note that $N_{\omega,\tau}(p,\varphi)$ has one maximum and one minimum in each range of π . The positions of these extrema are determined by a theorem which is a very simple extension of a theorem due to Newton.⁶ Differentiating $N_{\omega,\tau}(p,\varphi)$ in Eq. (10) we get

$$\frac{dN_{\omega,\tau}(p,\varphi)}{d\varphi} = -\frac{1}{\omega\tau} N_{0,\tau}(p,\varphi) - \frac{1}{\omega\tau} N_{\omega,\tau}(p,\varphi),$$

and at an extremum

$$N_{0,\tau}(p,\varphi_{\text{extr.}}) = N_{\omega,\tau}(p,\varphi_{\text{extr.}}), \quad (11)$$

which means that both the maxima and the minima of $N_{\omega,\tau}(p,\varphi)$ lie on $N_{0,\tau}(p,\varphi)$.

The ratio R of the maximum values of $N_{\omega,\tau}(p,\varphi)$ to the minimum values depends on τ and can therefore be used as a direct measurement of τ if the dependence of τ on R is known. The function $\tau(R)$ depends, of course, on the shape of $N_{0,\tau}(p,\varphi)$. We analyze in detail the case where $N_{0,\tau}(p,\varphi)$ is given by a Gaussian:

$$N_{0,\tau}(p,\varphi) = N \exp(-\varphi^2/a^2),$$

where we assume that p corresponds to the maximum of a peak in the spectrum $S(p)$, since this corresponds to the procedure adopted in the measurements.

$N_{\omega,\tau}(p,\varphi)$ is given in the interval $(-\pi/2 \dots \pi/2)$ by

$$N_{\omega,\tau}(p,\varphi) = N' e^{-\varphi/\omega\tau} \left[1 + \Phi\left(\frac{\varphi}{a} - \frac{a}{2\omega\tau}\right) + \frac{2e^{-\pi/\omega\tau}}{1 - e^{-\pi/\omega\tau}} \right], \quad (12)$$

where $N' = N(a\sqrt{\pi}/2\omega\tau) \exp[(a/2\omega\tau)^2]$ and $\Phi(\sigma)$ is the

⁶ T. D. Newton, Phys. Rev. 78, 490 (1950).

error integral $(2/\sqrt{\pi})\int_0^a \exp(-x^2)dx$. In the derivation of (12) the further assumption has been made that $a \ll \pi$. The value of R for the function (12) is given in Fig. 4 as a function of $\omega\tau$ for various values of a .

The analysis of τ in terms of R in the simple manner described above is of course possible only if the "periodicity" [Eq. (5)] is valid.

PHASE RESOLUTION AND DUTY CYCLE

The phase resolution r_φ of the modulating system is defined as the full width at half maximum of the function $N_{0,\tau}(p,\varphi)$, if p corresponds to the peak of some electron line. The phase resolution depends on one hand on the amplitude of the oscillation—the quantities b and q , and on the other hand on the line-widths—the width of the function $G(x)$ [which is made up of the size of the slit D and the size of the beam spot as given by the function $g(x)$] and the width of $S(p)$ —the spectral line. If the full width at half maximum of $G(x)$ is denoted by Δx and that of S by Δp and if these widths are narrow:

$$\Delta x/b \ll 1, \quad \Delta p/q \ll 1,$$

then we have

$$r_\varphi = \{a_b(\Delta x/b)^2 + a_q(\Delta p/q)^2\}^{\frac{1}{2}}, \quad (13)$$

where a_b, a_q are numerical constants depending on the shape of the distributions. If in particular both $G(x)$ and $S(p)$ are Gaussian then one gets from Eq. (13)

$$r_\varphi = \{(\Delta x/b)^2 + (\Delta p/q)^2\}^{\frac{1}{2}}. \quad (13a)$$

A quantity closely related to the phase resolution is the duty cycle d_c . For the beam cavity this is defined as the ratio of the average modulated current on the target to the unmodulated current, and for the spectrometer cavity it is defined as the ratio of the counting rate in the spectrometer with and without electron energy modulation, assuming the spectrometer setting to correspond to the peak of an electron line. In our arrangement these two duty cycles were equal as this appears to be the most advantageous combination. In what follows the term duty cycle will be used for this common value.

The duty cycle most suitable to the experiment is determined by a compromise between two considerations: to improve the phase resolution the duty cycle has to be decreased, whereas high counting rates require a large duty cycle. Considerations of counting rates are more critical in this type of measurement than in conventional beam pulsing experiments in the 10^{-9} sec range⁷ for two reasons:

(a) The method of timing by means of phase variation requires that the measurement at each phase point be carried out separately, whereas with electronic timing devices it is possible to cover the complete

time spectrum simultaneously. In other words, the counting rate is proportional to the square of the duty cycle.

(b) The targets have to be thin enough to avoid excessive momentum spread of the conversion electrons. Our targets were 5–10 kev thick for protons of 2.5 Mev, producing electron momentum spreads of the same order as the resolution of the β -ray spectrometer.

The duty cycle adopted throughout the experiment (with one exception mentioned later in the text) was $1/7$. The operational details corresponding to this value are those mentioned earlier, with 30-watt dissipation in each cavity.

The duty cycle is closely connected with the phase resolution; if $\Delta x/b \ll 1$, $\Delta p/q \ll 1$, and if $G(x)$ and $S(p)$ are Gaussian, then

$$r_\varphi = 2(2\pi \ln 2)^{\frac{1}{2}} d_c = 4.15 d_c. \quad (14)$$

For $d_c = 1/7$ one gets $r_\varphi = 0.59$.

TIME RESOLUTION

In a modulation measurement with angular frequency ω , the phase resolution r_φ gives rise to a time resolution r_t :

$$r_t = r_\varphi / \omega.$$

If in addition to the broadening due to the finite duty cycle there is a broadening caused by imperfect timing in any part of the system represented by a normalized function $f(t)$, then this will produce an additional time uncertainty \bar{r}_t equal to the width of $f(t)$ which is independent of ω , and the over-all time resolution R_t will then be a function of both r_φ and \bar{r}_t . For Gaussian distributions in particular:

$$R_t = \{(r_\varphi/\omega)^2 + \bar{r}_t^2\}^{\frac{1}{2}}, \quad (15)$$

and this in turn is equivalent to an over-all phase resolution R_φ given by

$$R_\varphi = \{r_\varphi^2 + \omega^2 \bar{r}_t^2\}^{\frac{1}{2}}. \quad (16)$$

Under these conditions the measured function $\bar{N}_{\omega,\tau}(p,\varphi)$ is different from the function $N_{\omega,\tau}(p,\varphi)$ defined in Eq. (7). Instead of Eqs. (9), (10) one gets the relations:

$$\bar{N}_{\omega,\tau}(p,\varphi) = \int_{-\infty}^{\infty} \bar{N}_{\omega,0}(p,\varphi') \frac{e^{-(\varphi-\varphi')/\omega\tau}}{\omega\tau} d\varphi', \quad (17)$$

where

$$\bar{N}_{\omega,0}(p,\varphi) = \int_{-\infty}^{\infty} \bar{N}_{0,\tau}(p,\varphi') f\left(\frac{\varphi-\varphi'}{\omega}\right) \frac{d\varphi'}{\omega} \quad (18)$$

and

$$\bar{N}_{0,\tau}(p,\varphi) = N_{0,\tau}(p,\varphi).$$

For Gaussian distributions $\bar{N}_{\omega,0}(p,\varphi)$ has a total width $R_\varphi = \{r_\varphi^2 + \omega^2 \bar{r}_t^2\}^{\frac{1}{2}}$, whereas for $\bar{N}_{0,\tau}(p,\varphi)$, $R_\varphi = r_\varphi$.

In our experiment a time broadening $f(t)$ was produced by variation in the transit time of the protons between the two cavities. The transit time t is given

⁷ M. Birk, G. Goldring, and Y. Wolfson, Phys. Rev. **116**, 730 (1959).

by l/v where l is the distance traversed by the protons between the cavities and v the velocity of the protons. We have

$$dt/t = dl/l - dv/v.$$

In our arrangement t was $\sim 10^{-7}$ sec, and therefore (writing \bar{r}_t' for dt)

$$\bar{r}_t' = (dl/l - dv/v)10^{-7} \text{ sec.} \quad (19)$$

Equation (19) gives the time spread produced by variations in the path length and velocity of the protons.

The velocity spread in the proton beam entering the deflection cavity is due to the limited energy stability of the accelerator. The energy spread in our experiments was $\Delta E/E = 0.0015$, producing a velocity spread: $\Delta v/v = 0.0007$. This gives according to Eq. (19) a time spread of 7×10^{-11} sec, which is large enough to preclude the possibility of accurate measurements in the range of 10^{-11} sec. In order to decrease this spread, we make use of the fact that after a proton enters the deflection magnet the velocity of the proton determines its path and therefore also l as a function of v . Assuming an infinitely narrow beam the geometry of the system can now be adjusted in such a way that the function $l(v)$ will satisfy the equation:

$$dl/l - dv/v = 0.$$

This condition is satisfied to a first approximation if the target is set at an angle α to the proton beam. For a 90° deflection magnet $\tan \alpha = 1 + l_1/(\rho + L)$, where l_1 is the distance between the deflection cavity and the magnet, ρ the radius of curvature in the magnet, and L the distance from the magnet to the target. With such a tilted target (which also implies a tilted spectrometer) one may expect a greatly reduced \bar{r}_t' . There is, however, a limit to this reduction because the dependence of the proton path on v is completely determined only if the proton beam is strictly parallel. As a result of the finite extension of the diaphragms, scattering, and space charge effects protons of the same velocity may move along different paths or vice versa, protons along the same path may have different velocities. If Δx is the beam width at the position of the target determined by these aberrations, then the additional time spread introduced is

$$\bar{r}_t'' = (\Delta x/l) \tan \alpha \times 10^{-7} \text{ sec.}$$

Combining \bar{r}_t' and \bar{r}_t'' one gets

$$\bar{r}_t(v) = (\bar{r}_t'^2 + \bar{r}_t''^2)^{1/2} \\ = \frac{1}{l} \left[\left(\tan \alpha - l - \frac{l_1}{\rho + l} \right)^2 \Delta s^2 + \Delta x^2 \tan^2 \alpha \right]^{1/2} \times 10^{-7} \text{ sec,}$$

where Δs is the width of the stabilizing slit. This expression is minimum for

$$\cot \alpha = \frac{L + \rho}{l_1 + L + \rho} \left(1 + \frac{\Delta x^2}{\Delta s^2} \right).$$

In the present arrangement the parameters were $l_1 = 60$ cm, $L + \rho = 140$ cm, and $\Delta x/\Delta s \sim 0.3$. For these dimensions one gets $\alpha = 52^\circ$. For practical reasons the tilting angle was chosen 45° . For this value of α one gets

$$\bar{r}_t(v) \approx 2.3 \times 10^{-11} \text{ sec.}$$

A spread in l is also produced by the finite size of the beam as it enters the deflection magnet. In principle the broadening $\bar{r}_t(l)$ produced by this spread can also be reduced to zero by a proper spacing between the tilted target and the focal point of the beam in the plane of deflection. The position of this "transverse" focal point is however exceedingly difficult to establish and therefore the geometrical adjustment can be carried out only very approximately. In any case $\bar{r}_t(l)$ is expected to be rather small and we believe that it is not bigger than 0.5×10^{-11} sec:

$$\bar{r}_t(l) \leq 0.5 \times 10^{-11} \text{ sec.}$$

Finally there is the spread produced by the magnet itself. The magnetic field is stabilized to $\pm 5 \times 10^{-5}$ producing a time spread:

$$\bar{r}_t(\text{mag}) \sim 10^{-11} \text{ sec.}$$

Combining the various spreads, we get for the over-all time uncertainty:

$$\bar{r}_t = \{\bar{r}_t(v)^2 + \bar{r}_t(l)^2 + \bar{r}_t(\text{mag})^2\}^{1/2} \sim 2.6 \times 10^{-11} \text{ sec.} \quad (20)$$

The value given in (20) is only a rough estimate, since the optical properties of the beam on which \bar{r}_t depends are neither well known nor properly controllable. The proton beam optics constitutes indeed the essential limitation on the accuracy and the scope of measurements of the type presented here.

The longitudinal components of the electric field produced in the deflection cavity modify the energy distribution of the protons within the beam.⁸ This energy spread as well as all other energy variations in the proton beam before the magnet are compensated for by the combination of deflection magnet and tilted target.

TARGET PREPARATION

The targets were prepared by evaporation of separated isotopes in the form of oxides on nickel backing of $125 \mu\text{g cm}^{-2}$. The evaporation was carried out by placing the target material in a small graphite cup and bombarding it with 10–50 ma of electrons accelerated to 5 kv. The targets proved completely stable under proton bombardment with currents up to $1 \mu\text{a}$. On analysis in the β spectrometer no broadening of the lines (and only a very insubstantial shift) could be detected after 50 hours of bombardment. The targets were $100\text{--}200 \mu\text{g cm}^{-2}$ thick.

⁸ T. K. Fowler and W. M. Good, Nuclear Instr. 7, 245 (1960)

DESCRIPTION OF THE MEASUREMENTS

Tm^{169}

The β spectrum of Tm^{169} is shown in Fig. 5. The peak corresponds to K -conversion electrons from the 110-keV transition. The "background" is largely due to δ rays. Such a large background would make the modulation measurement rather insensitive and therefore two NaI crystal counters were placed behind the target and set to record K x-rays in coincidence with the electrons. The total efficiency of these counters was $\sim 8\%$. It is evident from Fig. 5 that the background is very much reduced by this arrangement. The reduction is caused by the fact that in this range of electron energies the δ -ray electrons come mainly from outer shells and the K x-rays coincidence requirement discriminates against them very efficiently.

A measurement of the prompt phase distribution function $\bar{N}_{0,\tau}(p_0, \varphi)$ [or rather $\bar{N}_{100\pi,\tau}(p_0, \varphi)$] was carried out by setting the spectrometer to the peak value p_0 and modulating the spectrometer current sinusoidally with 50 cycles/sec. At the same time the proton beam was swept with the same frequency by applying a sinusoidal voltage to a pair of deflection plates. The beam pulsing and the spectrometer modulation were both adjusted to duty cycles $d_c=1/7$ [see Figs. 8, 9(a), 9(b)]. The 50-cycle/sec modulation differs from the microwave modulation in two respects: (a) The spectrometer setting is changed in the 50 cycle/sec modulation, keeping the electron energy constant, rather than modulating the electron energy and keeping the spectrometer current fixed. This difference is obviously of no consequence. (b) The 50-cycle/sec modulation is linear in the momentum

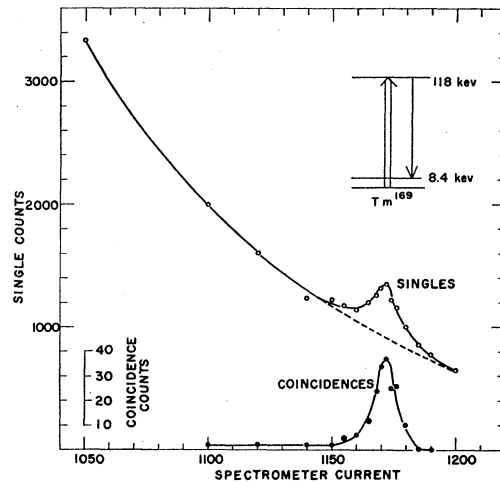
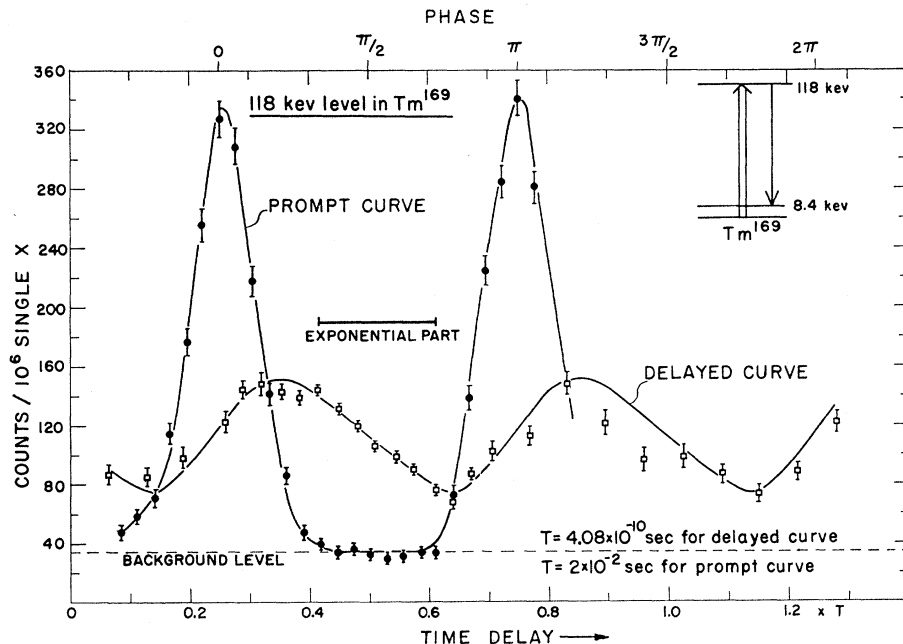


FIG. 5. Electron spectrum from a Tm^{169} target in the neighborhood of the K -conversion line of the 110-keV transition from the 118-keV level to the 8.4-keV level. The curve marked "coincidence" shows the spectrum of electrons in coincidence with K x-rays.

$p = p_0 + q \sin \omega t$, whereas the microwave modulation is linear in the energy of the electrons. It has already been pointed out that these two procedures are equivalent if the amplitude of modulation is small. Figure 6 shows the curve obtained for the number of (coincidence) counts as a function of phase angle. The counts were taken for a fixed number of single counts in the x-ray counter. The symmetry with respect to the peak [Eq. (4)] and the π periodicity [Eq. (5)] (both the current distribution function and the conversion line spectrum were symmetric) are evident from the figure. In particular we note that as a consequence of the

FIG. 6. The functions $\bar{N}_{0,\tau}(p_0, \varphi)$ (marked "prompt") and $\bar{N}_{\omega,\tau}(p_0, \varphi)$ (marked "delayed") for the 110-keV transition in Tm^{169} , as a function of phase angle φ . p_0 is the spectrometer setting corresponding to the peak of the K -conversion line. The 'counts' are coincidence counts between electrons and x rays and all counts are given per 10^6 counts in the x-ray counter.



symmetrization the background is constant (independent of φ), although the background in the spectrum proper $S(p)$ (Figs. 5, 8) is asymmetric.

The "delayed" phase distribution function $\bar{N}_{\omega,\tau}(p_0,\varphi)$ ($\omega = 2\pi \times 2.45 \times 10^9$ rad sec $^{-1}$) was measured by applying the microwave fields to the beam and to the electrons. The 50-cycle/sec and the microwave modulations were matched by setting the amplitudes of oscillation to the same duty cycle. The microwave phase was controlled by changing the field of the deflection magnet (and thereby the velocity of the protons) and the counts were again taken for a fixed number of single x-ray counts. In Fig. 6 the number of coincidence counts, both prompt and delayed, are given per 10^6 single x-ray counts. The only arbitrariness in the relation of the two distribution functions is, in practice, the relative phase for the two oscillation frequencies. It is almost impossible to establish by a direct measurement the phase relationship between the two measurements. In a series of measurements comprising several transitions one could in principle establish the phase relationship once and for all in *one* case, by fitting the distribution functions, and then use this as a standard.

In Fig. 6 the phases were fitted by making $\bar{N}_{0,\tau}(p_0,\varphi)$ go through the minima of $\bar{N}_{\omega,\tau}(p_0,\varphi)$ as required by Eq. (11). The maxima of $\bar{N}_{\omega,\tau}(p_0,\varphi)$ do not quite coincide with $\bar{N}_{0,\tau}(p_0,\varphi)$ but are at slightly larger distances from the minima. This shows that the "true prompt" distribution $\bar{N}_{\omega,0}(p_0,\varphi)$ is slightly wider than the 50-cycle prompt distribution $\bar{N}_{0,\tau}(p_0,\varphi)$ [see Eqs. (16), (17), and (18)]. The complete measurement required about 50 hours, with a mean modulated beam current of $0.3 \mu\text{a}$.

We now turn to the question of the determination of τ from the measurements. The background can be subtracted very accurately from $\bar{N}_{\omega,\tau}(p_0,\varphi)$ because it is independent of ω and therefore equal to the background of $\bar{N}_{0,\tau}(p_0,\varphi)$ which, as we have seen, is quite

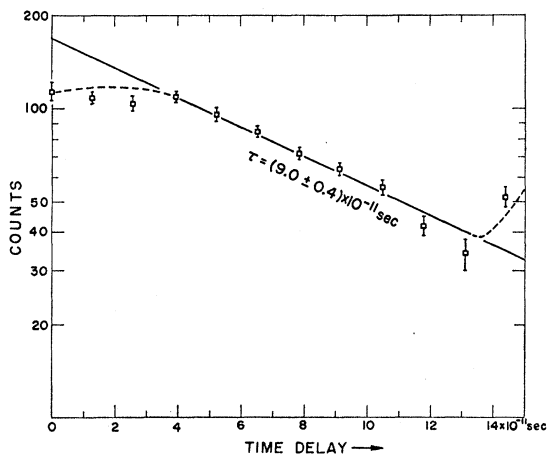


FIG. 7. The exponential decay of the 118-keV level of Tm^{169} .

unambiguously defined. After subtracting the background from both $\bar{N}_{\omega,\tau}(p_0,\varphi)$ and $\bar{N}_{0,\tau}(p_0,\varphi)$ one could attempt to unfold the exponential decay curve from $\bar{N}_{\omega,\tau}(p_0,\varphi)$ and $\bar{N}_{0,\tau}(p_0,\varphi)$ with the aid of Eqs. (17), (18) or use some equivalent method like the determination of the ratio R of the maximum value of $\bar{N}_{\omega,\tau}(p_0,\varphi)$ to its minimum value. All such procedures are essentially inaccurate because the relation between $\bar{N}_{0,\tau}(p_0,\varphi)$ and the "true prompt" distribution function $\bar{N}_{\omega,0}(p_0,\varphi)$ is not known well enough. However, we notice that the function $\bar{N}_{0,\tau}(p_0,\varphi)$ is zero over an appreciable range of phases (equivalent to $\sim 8 \times 10^{-11}$ sec). In this range $\bar{N}_{\omega,\tau}(p_0,\varphi)$ should be strictly exponential: $e^{-\varphi/\omega\tau}$. In Fig. 7, $\bar{N}_{\omega,\tau}(p_0,\varphi)$ is drawn on a

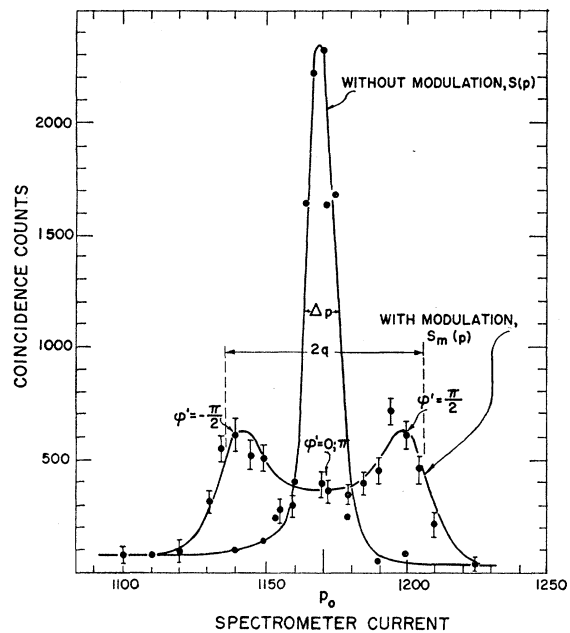


FIG. 8. The effect of the electron momentum modulation on the spectrum of the K -conversion line of the 110-keV transition in Tm^{169} . The duty cycle is the ratio of counts with and without modulation with the spectrometer setting at the peak value p_0 , and is seen from the figure to be $\sim 1/7$.

logarithmic scale (after background subtraction), and the exponential decay is quite evident. The value of the mean life τ is found from a least-squares fit to be $(9.0 \pm 0.4) \times 10^{-11}$ sec, in close agreement with an earlier measurement [$\tau = (9.0 \pm 1.4) \times 10^{-11}$ sec] carried out with a two-spectrometer coincidence arrangement.⁴ The determination of the mean life directly from the exponential decay is a very satisfactory procedure, primarily because no detailed knowledge of the prompt distribution function is required, but also because quite generally this is the most straightforward and dependable way of measuring decay constants.

The time delay in Fig. 6 is determined by the relation $dt = -(l/v)(dv/v)$, where l is the length of the path traversed by the protons between the two cavities and

v is the proton velocity. The period of the measured function $\bar{N}_{\omega,\tau}(\rho_0, \varphi)$ is found, as expected, to be $T/2$, where T is the period of the microwave oscillations ($T=40.8 \times 10^{-11}$ sec).

It is an attractive feature of this type of time measurement that it is possible in principle to calibrate the time scale *directly* by means of the microwave period, if the period of $\bar{N}_{\omega,\tau}(\rho_0, \varphi)$, φ_T , is used as a phase standard: $\varphi_T = \pi$.

In order to clarify the effect of the microwave modulation on the electron spectrum, the spectrum of the K line of the 110-kev transition in Tm^{169} (coincidence counts vs spectrometer current) is shown in Fig. 8 with and without microwave modulation. The modulated spectrum is represented by the function $S_m(\rho)$:

$$S_m(\rho) = \frac{1}{\Theta} \int_{-\Theta/2}^{\Theta/2} S_i(\rho, t) dt,$$

where $S_i(\rho, t)$ is the instantaneous spectrum [see Eq. (2)],

$$S_i(\rho, t) = S(\rho - q \sin(\omega t - \varphi)),$$

and $S(\rho)$ is the unmodulated spectrum. φ is an arbitrary phase in this case, and $S_m(\rho)$ is independent of φ .

There is a correlation in the modulated spectrum between the spectrometer setting ρ and the microwave phase. If we neglect the width of $S(\rho)$ and assume $S(\rho) \sim \delta(\rho_0)$, we find that electrons counted at the setting ρ have gone through the cavity at a phase φ' given by

$$\rho = \rho_0 + q \sin \varphi',$$

where we have put $\varphi' = \omega t - \varphi$, so that $\varphi' = 0$ at the moment the accelerating field is zero.

The sharpness with which the phase is defined—the phase resolution—is essentially determined by the ratio of the momentum resolution $\Delta\rho$ to the amplitude of modulation q .

The effect of the modulation on the proton beam is similarly illustrated in Figs. 9(a), 9(b), representing the current passing the beam chopping slit as a function of slit position. In practice the slit was fixed and the change in position was simulated by applying a variable deflection field to the beam. Figure 9(a) represents the apparent beam profile $G(x)$ [see Eq. (1)] and Fig. 9(b) is the profile of the modulated beam $G_m(x)$:

$$G_m(x) = \frac{1}{\Theta} \int_{-\Theta/2}^{\Theta/2} G(x - b \sin \omega t) dt.$$

The beam position coordinate x is again correlated with the microwave phase and the sharpness of the phase definition is determined by the ratio of the width of $G(x)$ (which is a combination of the beam width and the slit width) and the amplitude of modulation b . The over-all phase resolution r_φ (the width of the “prompt” curve in Fig. 6) is a combination of the phase

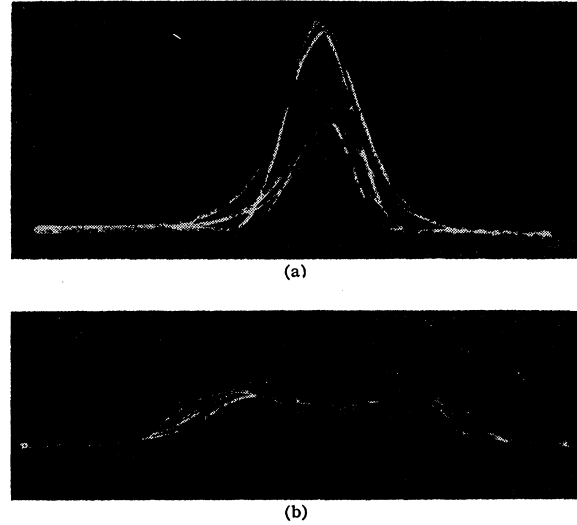


FIG. 9. (a) The apparent beam profile $G(x)$. The oscillogram was obtained by feeding to the vertical plates of an oscilloscope a signal which is proportional to the current falling on a plate placed behind the beam chopping slits, and to the horizontal plates a signal proportional to the field which deflects the beam across the slit. (b) As in (a), with proton beam modulating cavity in operation. The duty cycle is the ratio of currents with and without modulation with zero deflection field [peak position in (a) and minimum position in (b)]. For the currents represented by Figs. 9(a), 9(b) the duty cycle is found to be $\sim 1/7$.

broadening in both the proton beam and the electron momentum modulations.

Lu^{175} , Hf^{179} , Ta^{181}

The mean lives of the first excited states of Lu^{175} , Hf^{179} , and Ta^{181} were measured and analyzed in the same manner as Tm^{169} . The decay curves are shown in Figs. 10, 11, and 12 and the results are summarized in Table I.

With the values of the mean lives of the levels of Tm^{169} , Lu^{175} , Hf^{179} , and Ta^{181} well established, an attempt was made to analyze the time resolution of the apparatus in some detail. The ratios R for Tm, Hf, Lu, and Ta were found to be 3.0, 2.0, 5.8, and 4.1, respectively. From these values of R one can, with the aid of Fig. 4, determine the mean lives, provided the time resolution R_t is known. With the assumption that R_t is completely given by the width of the “prompt” distribution function $\bar{N}_{\omega,\tau}(\rho, \varphi)$, one has $R_t = r_\varphi / \omega = 5.3 \times 10^{-11}$ sec, and with this value of R_t one gets values for the mean lives which are consistently too high. If, on the other hand, one tries to determine the value R_t which will give the correct values for the mean lives one finds $R_t = 6.1 \times 10^{-11}$ sec. With this value of R_t the calculated values for all three mean lives are within 10% of the measured values. From Eq. (15) we now get

$$\bar{r}_t = (3 \pm 1) \times 10^{-11} \text{ sec.} \quad (20a)$$

The error 1×10^{-11} sec reflects the uncertainty in the

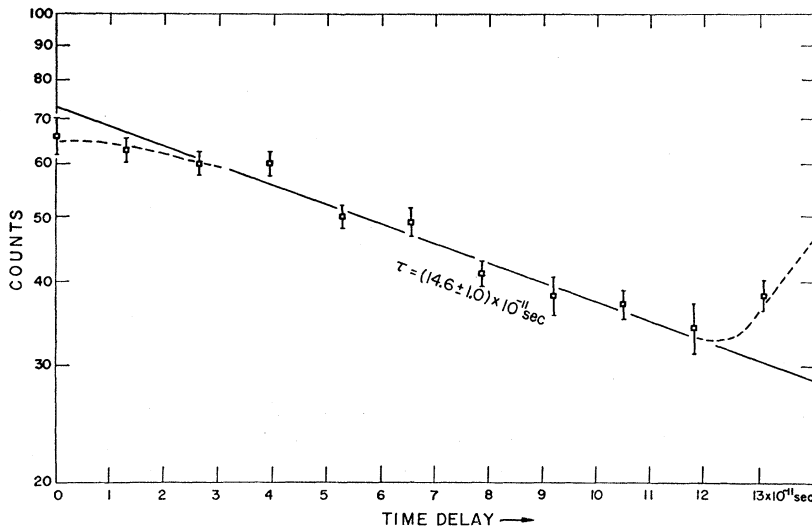


FIG. 10. The exponential decay of the 113-keV level of Lu^{175} .

value of R_t . This value of $\bar{\tau}_t$ is in good agreement with the estimate made in (20). The value $R_t = 6.1 \times 10^{-11}$ sec is also consistent with the spacings of the minima and maxima in the delayed distribution function for Tm^{169} .

Re^{185} , Re^{187}

The prompt and delayed distribution function for the first excited state in Re^{185} is shown in Fig. 13. For Re^{187} almost identical functions were obtained. These levels are evidently much shorter lived than all the levels discussed before. One cannot hope to observe the exponential decay of such fast transitions, nor can the ratio R be used for a determination of τ because R is too large and too uncertain. From the slope of the delayed distribution functions an upper limit for the lifetimes can be established. In this way one obtains for both isotopes $\tau \leq 2.4 \times 10^{-11}$ sec. The width of the delayed distribution functions is 6.3×10^{-11} sec. This

constitutes an absolute upper limit for the width of the true prompt distribution function $\bar{N}_{\omega,0}(p, \varphi)$. In particular one gets an upper limit for the inherent time spread: $\bar{\tau}_t \leq 3.5 \times 10^{-11}$ sec, where the limiting value 3.5×10^{-11} sec corresponds to $\tau(\text{Re}) = 0$. The estimate of $\bar{\tau}_t$ given in Eq. (20a) is consistent with this limit.

Hf^{177}

The magnetic transition probabilities in Hf^{177} are known to be small⁹ and therefore the mean life of the first excited state is expected to be rather long. Another consequence of the small value of the ratio $M1/E2$ is that the ratio of K to L conversion is smaller than in the transitions previously discussed, which were all predominantly $M1$. It therefore turned out to be preferable in this case to work with L -conversion electrons (without the coincidence arrangement) rather than with K -conversion electrons as above. At the energy of the L -conversion line the number of δ -ray

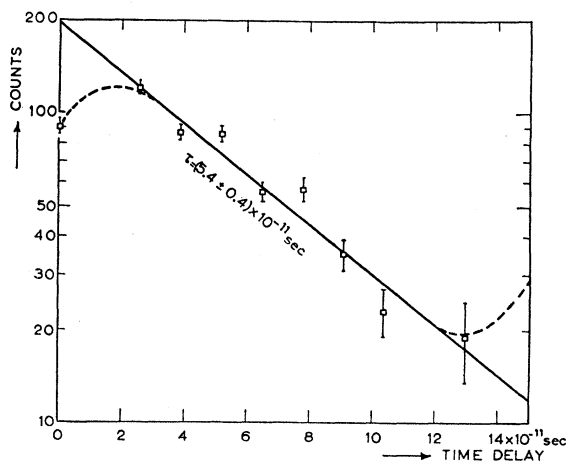


FIG. 11. The exponential decay of the 122-keV level of Hf^{179} .

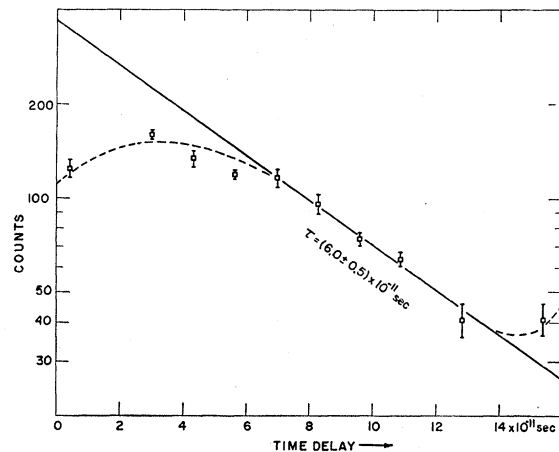


FIG. 12. The exponential decay of the 136-keV level of Ta^{181} .

electrons is insignificant and no appreciable background is observed in the electron spectrum. However, modulating L -conversion electrons has the drawback that only a limited phase resolution can be achieved: On the one hand, there are three L lines, introducing a finite "width" and on the other hand the modulation amplitude cannot exceed the spacing between the L lines and the M lines. There is therefore a limiting phase resolution which for Hf^{177} is ~ 0.6 , corresponding to a time resolution of $\sim 4 \times 10^{-11}$ sec. In our measurement the over-all phase resolution was found to be 0.95, corresponding to a time resolution of 6.1×10^{-11} sec. The duty cycle was in this case $\frac{1}{3}$ (instead of $1/7$ in the other measurements).

The prompt and delayed distribution functions for the first excited level in Hf^{177} are shown in Fig. 13. In this case the background had to be deduced from the unmodulated electron spectrum. It is obvious from the figure that the microwave period is too short for this transition, and only a rough estimate can be made. Assuming again that the inherent instrumental time resolution is 3×10^{-11} sec we get for the over-all resolution: $R_t = 7 \times 10^{-11}$ sec. With this value one gets from the ratio R ($R = 1.13$) corresponding to the line drawn out in Fig. 14: $\tau = (70 \pm 8) \times 10^{-11}$ sec. The error is due to the limited accuracy of the present evaluation of the function $R(\omega\tau)$ in the region $\tau > T$. The line in Fig. 14 is extremal in the sense that R is certainly not larger than 1.13 but it may well be smaller and therefore the value for τ derived above can only be taken as a lower

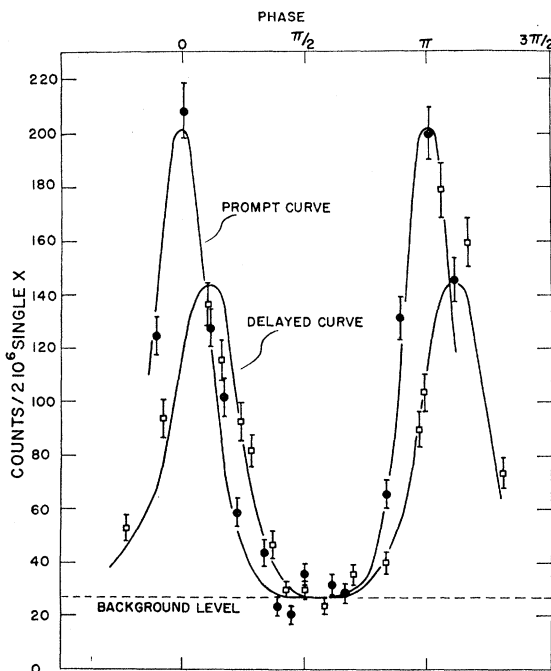


FIG. 13. The function $\bar{N}_{0,\tau}(p_0, \varphi)$ ("prompt") and $\bar{N}_{\omega,\tau}(p_0, \varphi)$ ("delayed") for the 126-keV transition in Re^{185} .

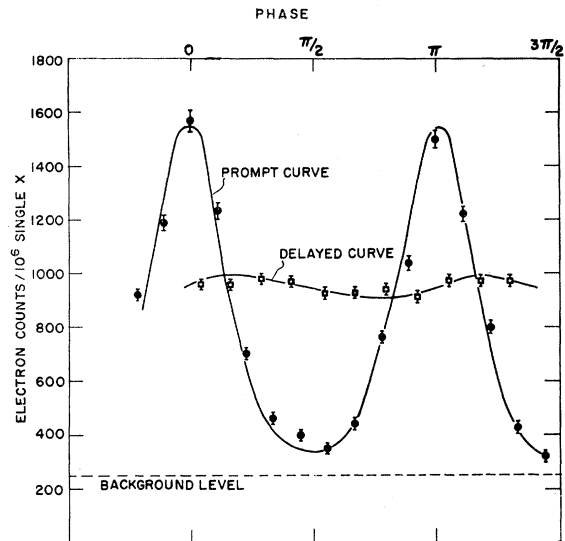


FIG. 14. The functions $\bar{N}_{0,\tau}(p_0, \varphi)$ ("prompt") and $\bar{N}_{\omega,\tau}(p_0, \varphi)$ ("delayed") for the 113-keV transition in Hf^{177} . p_0 is the spectrometer setting corresponding to the peak of the L -conversion line.

limit:

$$\tau \geq 60 \times 10^{-11} \text{ sec.}$$

From the Coulomb excitation cross section⁹ one gets the partial lifetime for $E2$ as $\tau_{E2} = (60 \pm 20) 10^{-11}$ sec. The ratio $\delta^2 = E2/M1$ is therefore large. In this case (of large δ^2) the lifetime measurement is equivalent to a measurement of the $B(E2)$ value (e.g., by Coulomb excitation methods). The determination of $B(M1)$ necessitates in both cases an exact evaluation of the mixing ratio δ^2 .

DISCUSSION OF THE RESULTS

The results of the lifetime measurements are summarized in Table I. In this table are also given the values of the K/L ratio which were measured for all the nuclei investigated except Ta^{181} and Re^{187} , in which the L -conversion electrons have energies too high for our spectrometer. Previous measurements of K/L ratios⁹ are rather inconsistent and the present measurements are also in disagreement with at least parts of previous sets of measurements. The values of σ^2 were determined from the K/L ratios given in column 4. For Ta^{181} and Re^{187} for which measurements of δ^2 have not been carried out, δ^2 was computed from Coulomb excitation data on $B(E2)$ values.

The $B(M1)$ values given in the seventh column of Table I were computed from the measured mean lives

⁹ T. Huus *et al.*, Kgl. Danske Videnskab. Selskab, Mat.-fys. Medd. **30**, No. 17 (1956); E. M. Bernstein and E. H. Lewis, Phys. Rev. **105**, 1524 (1957); E. M. Bernstein, Phys. Rev. **112**, 2026 (1958).

TABLE I. Summary of results. τ and K/L are the values measured in the present work. δ^2 is the ratio $E2/M1$ computed from the measured values of K/L . $B(M1)$ are the reduced $M1$ transition probabilities in units of $(e\hbar/2Mc)^2$. The values g_R , g_Ω were computed according to Bohr and Mottleson^a, from the values of $B(M1)$ derived from the lifetime measurements and the magnetic moments μ of the ground states. The errors quoted include the experimental errors in the measurements of $B(M1)$ and μ .

1	2	3	4	5	6	7	8	9	10	11
Nucleus	Transition energy in keV	Mean life τ in 10^{-11} sec	K/L	$\delta^2 = E2/M1$ from K/L	α from Sliv and Band ^b	$B(M1)$ from τ	$B(E2)$ and δ^2	μ from Noya <i>et al.</i> ^c	g_R	g_Ω
Tm ¹⁶⁹	110	9.0 ± 0.4	6.5 ± 0.5	≤ 0.04	2.45	0.121 ± 0.006	≥ 0.08	-0.205 ± 0.02	0.26 ± 0.06 ^d	-2.25 ± 0.14 ^d
Lu ¹⁷⁵	114	14.6 ± 1	3.2 ± 0.3	0.18 ± 0.06	2.74	0.060 ± 0.005	0.085 ± 0.03	2.0 ± 0.2 ^e	0.31 ± 0.05	0.65 ± 0.06
Hf ¹⁷⁷	113	≥ 60	0.42 ± 0.1	≥ 10	2.32	≤ 0.0025	≤ 0.0025	0.61 ± 0.03	0.20 ± 0.04	0.17 ± 0.02
Hf ¹⁷⁹	122	5.4 ± 0.04	4.5 ± 0.6	0.083 ± 0.015	2.31	0.162 ± 0.013	0.20 ± 0.08	-0.47 ± 0.03	0.28 ± 0.015	-0.19 ± 0.01
Ta ¹⁸¹	136	6.0 ± 0.5	...	0.20 ± 0.01 ^f	1.86	0.110 ± 0.010	0.12 ± 0.05	2.340 ^g	0.31 ± 0.015	0.77 ± 0.005
Re ¹⁸⁵	128	≤ 2.4	4.0 ± 0.5	0.13 ± 0.04	2.60	≥ 0.28	0.14 ± 0.05	3.1433 ± 0.0006	≤ 0.6	≤ 1.5
Re ¹⁸⁷	134	≤ 2.4	2.16	≥ 0.28 ^h	...	3.1755 ± 0.0006	≤ 0.6	≤ 1.5

^a See reference 1.

^b See reference 10.

^c See reference 12.

^d The decoupling parameter b_0 which appears in the analysis of $K = \frac{1}{2}$ bands is here assumed to be 0.1. This value was derived from experimental results given in references 4 and 11.

^e A. Steudel, *Naturwissenschaften* **49**, 371 (1957).

^f E. M. Bernstein (private communication).

^g L. H. Bennet and J. I. Budnik, *Bull. Am. Phys. Soc.* **5**, 417 (1959).

^h Assuming δ^2 to be the same as for Re¹⁸⁵.

through the relation:

$$\frac{1}{\tau} = \frac{16\pi}{9} \frac{1}{\hbar} \left(\frac{E_\gamma}{\hbar c} \right)^3 \left(\frac{e\hbar}{2Mc} \right)^2 (1+\alpha)(1+\delta^2)B(M1). \quad (21)$$

The conversion coefficients α were taken from Sliv.¹⁰

The decay of the 118-keV level in Tm¹⁶⁹ is complex: Most of the decays are through the 110-keV transition and a small fraction are pure $E2$ crossover transitions to the ground state. The relation between $B(M1)$ and the total mean life τ must be modified in this case to take into account the crossover transitions. If we denote by I the branching ratio: number of 110-keV transitions/number of all transitions, then $1/\tau$ in (21) must be replaced by: I/τ . The branching ratio I was computed from the measured branching ratio b' for γ transitions¹¹: $b' = 0.9$, and from the conversion coefficients for the two transitions.¹⁰

The $B(M1)$ values given in the eighth column were computed from the measured values of δ^2 and the $B(E2)$ values in reference 3.

The accuracy of the $B(M1)$ values for the higher transitions is as yet not good enough for a rigorous test of the description of the levels in terms of a rotational band. However, if one assumes that g_R and g_Ω are constant throughout the rotational band, they can be evaluated if the $B(M1)$ value of one transition and the static magnetic moment of one level are known. The values g_R , g_Ω in Table I are calculated from the measured values of τ and the values of the magnetic moments of the ground states.¹²

¹⁰ L. A. Sliv and I. M. Band, Leningrad Physico-Technical Institute Report, 1956 and 1958 [translation: Reports 57 ICC K1 and 58 ICC L1 issued by Physics Department, University of Illinois, Urbana, Illinois (unpublished)].

¹¹ E. N. Hatch *et al.*, *Phys. Rev.* **104**, 745 (1956).

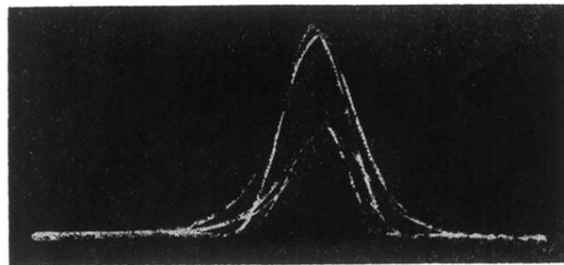
¹² H. Noya *et al.*, *Suppl. Progr. Theoret. Phys. (Kyoto)* **8**, 33 (1959).

DISCUSSION OF THE METHOD

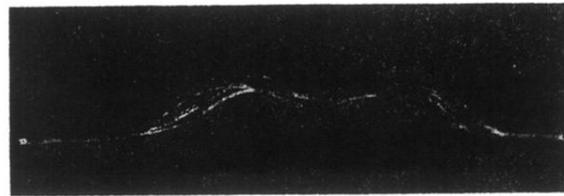
In conclusion, we would like to comment on the method here described as a whole, its scope and limitations. The most severe limitation is the requirement of conversion electrons which means that only low-lying levels and only medium and heavy nuclei can be investigated in this manner. In this region of nuclear levels, only those decaying by $M1$ radiation are fast enough to be outside the range of convenient electronic delay measurements and the $M1$ radiations have mean lives in the range of 0.5×10^{-11} – 20×10^{-11} sec. The determination of $M1$ transition probabilities for low-energy transitions in medium and heavy nuclei is therefore the natural task for microwave timing devices. The present system is limited to measurements in the range 5 – 40×10^{-11} sec; the upper limit is determined by the microwave period and could easily be raised if required. The lower limit is determined by the over-all time resolution and this in turn is limited by the inherent time spread due to the finite size of the proton beam spot. The inherent time spread can quite easily be reduced by a factor of two if the power in the beam deflection system is increased thereby reducing the flight path. Beyond that any improvement in resolution would require improved beam optics. The over-all time resolution also depends on the phase resolution and this is essentially determined by the microwave period, because the duty cycle is limited by requirements of counting rate. It therefore seems likely that for the very fast $M1$ transitions, 0.5 – 2×10^{-11} sec, an entirely new short-wave modulation system would have to be devised.

ACKNOWLEDGMENTS

Our sincere thanks are due to Mr. M. Loebenstein for the design and construction of the electron-bombardment evaporation unit, and to Mrs. S. Held for the spectroscopic analysis of our targets during all the stages of testing and target preparation.



(a)



(b)

FIG. 9. (a) The apparent beam profile $G(x)$. The oscillogram was obtained by feeding to the vertical plates of an oscilloscope a signal which is proportional to the current falling on a plate placed behind the beam chopping slits, and to the horizontal plates a signal proportional to the field which deflects the beam across the slit. (b) As in (a), with proton beam modulating cavity in operation. The duty cycle is the ratio of currents with and without modulation with zero deflection field [peak position in (a) and minimum position in (b)]. For the currents represented by Figs. 9(a), 9(b) the duty cycle is found to be $\sim 1/7$.